

Fractal geometry of Ising magnetic patterns: signatures of criticality and diffusive dynamics

E. Agliari¹, R. Burioni^{1,2}, D. Cassi^{1,2}, and A. Vezzani^{1,2}

¹ Università degli Studi di Parma, Parco Area delle Scienze 7/a, 43100 Parma, Italy

² Istituto Nazionale Fisica della Materia (INFN), UdR PARMA, Parco Area delle Scienze 7/a, 43100 Parma, Italy

Received: date / Revised version: date

Abstract. We investigate the geometric properties displayed by the magnetic patterns developing on a two-dimensional Ising system, when a diffusive thermal dynamics is adopted. Such a dynamics is generated by a random walker which diffuses throughout the sites of the lattice, updating the relevant spins. Since the walker is biased towards borders between clusters, the border-sites are more likely to be updated with respect to a non-diffusive dynamics and therefore, we expect the spin configurations to be affected. In particular, by means of the box-counting technique, we measure the fractal dimension of magnetic patterns emerging on the lattice, as the temperature is varied. Interestingly, our results provide a geometric signature of the phase transition and they also highlight some non-trivial, quantitative differences between the behaviors pertaining to the diffusive and non-diffusive dynamics.

PACS. 5.50.+q Lattice theory and statistics – 05.40.Fb Random walks and Levy flights – 05.45.Df Fractals

1 Introduction

In an earlier paper [1] we introduced a thermal dynamics for an Ising ferromagnet exhibiting a diffusive character: time evolution is performed by a walker which, according to a local probability, can hop across the sites of an underlying lattice and can possibly flip the relevant spins. In order to make such a dynamics consistent with some physical processes, which make the system evolve [1,2], the walker is biased towards high energy regions.

Due to a very general structure, our algorithm works as well for arbitrary lattices, made up of spins which can assume an arbitrary, finite number of states.

The thermodynamic effects of this thermal dynamics have already been explored [1], showing that, though the steady states reached by the system are non-canonical, the universality class is preserved. It was also noticed that the geometry of magnetic patterns developing on the lattice could be affected by the dynamics adopted. Indeed, due to the bias the walker is endowed with, we expect sites pertaining to boundaries between clusters to be more frequently updated. As a result, we also expect to have differently-shaped spin arrangements, with respect to a non-diffusive dynamics.

Hence, in this work, by inspecting the geometric properties of magnetic patterns, we aim to further deepen the study of the dynamics introduced. We underline that, while previous works dealing with the geometry of magnetic configurations [3,4,5,6,7,8,9] mainly concerned the analysis of the critical clusters (namely clusters emerging when $T = T_c$), here we are interested in how the diffusive

character of the dynamics influences the evolution of the spin arrangement on the whole lattice, as the temperature is varied.

An appropriate parameter to quantitatively describe clusters, in terms of geometric properties, is the fractal dimension [10,11,12]. Among the several methods introduced at this purpose [3,13,14,15,16], we select the box-counting technique which, as will be explained in Sec. 3, let us to easily achieve a complete description of the entire lattice. Moreover, as we will show, our geometric measures provide a significant signature of the critical point and, by a proper fit of data, we are also able to extract good estimates for T_c .

The same measures are performed on both spin-1/2 and spin-1 Ising systems, in order to achieve a wider insight into the matter and, possibly, to extend results to the general spin-S case. As discussed in the following, our results are strongly concerned with the symmetry existing among Ising spin-states, and, in fact, distributions of negative (positive) and null spins, display very different behaviors. In particular, as approaching T_c , the pertaining fractal dimension are described by a power and a linear law, respectively. Qualitatively analogous results are also obtained when a non-diffusive dynamics, with sequential spin-updating, is adopted. However, while the diffusive dynamics introduced recovers the canonical thermodynamics critical exponents [1], as far the geometric exponents, some interesting quantitative differences emerge.

The layout of the paper is as follows. In Sec. 2 we explain how our diffusive dynamics works, while in Sec. 3

we deal with the geometrical features, especially focusing on the critical range. Finally, Sec. 4 contains a summary and a discussion of results.

2 Diffusive Dynamics

In this Section we resume how the diffusive dynamics introduced works, while a detailed description can be found in [1].

Albeit our dynamics provides a versatile tool to be applied to an arbitrary spin- S discrete system, in this work we are focusing on spin-1/2 and spin-1 toroidal squared lattices, where only the exchange interaction is working. Hence, the related Hamiltonian can be written:

$$\mathcal{H} = -\frac{J}{S^2} \sum_{i \sim j}^N \sigma_i \sigma_j, \quad (1)$$

where S is the spin magnitude (the spin variable σ takes the $2S + 1$ pertinent values) and the sum only involves nearest-neighbor pairs.

The walker performing the dynamics can move on the magnetic lattice by hopping from one site to its nearest-neighbor and it can also flip the relevant spin. Notice that, as in the usual dynamics, the magnetic configuration of the lattice may remain unaltered during one or more steps. In fact, the walker is endowed with a non-null waiting probability and the spin-flip is only probable. In particular, the walker is ruled by the following (anisotropic) probability:

$$\mathcal{P}_T(\mathbf{s}, i, j) = \frac{p_T(\mathbf{s}, j)}{\sum_{\{\mathbf{s}'\}} \sum_{j=0}^{z_i} p_T(j, \mathbf{s}')}, \quad (2)$$

which represents the probability that the walker, from site i (with coordination number z_i), jumps on a n.n. site j , being \mathbf{s} the magnetic configuration attained at the step considered. At each step, the set of all the possible magnetic configurations (denoted as $\{\mathbf{s}'\}$) contains $(2S+1) \times (z_i+1)$ elements. Hence, \mathbf{s} represents a particular element from $\{\mathbf{s}'\}$. Furthermore,

$$p_T(j, \mathbf{s}) = \frac{1}{1 + e^{[\beta \Delta E_j(\mathbf{s})]}} \quad (3)$$

is drawn from the usual Glauber probability where $\Delta E_j(\mathbf{s})$ is the energy variation consequent to the process [1].

As a consequence of Eq. 2, the random walker is biased (BRW) towards such sites that let, by means of spin-flip, a greater energy gain.

Notice that, as stressed in [1], this kind of dynamics does violate the detailed balance condition and the equilibrium states achieved are non-canonical. More precisely, our diffusive dynamics can attain the actual thermodynamic behavior of the Ising ferromagnet, even if shifted to higher temperatures. In particular, the phase-transition occurs at temperatures

$$T_c^{S=1/2} = 2.602(1) \quad (4)$$

$$T_c^{S=1} = 1.955(2) \quad (5)$$



Fig. 1. These figures show a 75×75 zoom of the snapshots of typical magnetic configurations for a 400×400 spin-1/2 Ising lattice with $\langle m \rangle = 0.84$ subject to the Glauber dynamics at $T = 2.09$ (left panel) and to a diffusive one at $T = 2.40$ (right panel). The smallest (black) perturbations away from the ordered (white) background involve just a single site. Notice that the same magnetization is attained for different temperatures and also that, due to the diffusive character of the pertinent dynamics, the right figure displays a greater number of black islands, though smaller.

larger than the canonical ones. On the other hand, the universality class is preserved, i.e. the right critical exponents (relatively to the 2-dimensional case) are recovered with great accuracy. Finally, we recall that the critical temperatures relevant to a non-diffusive dynamics are, respectively, $T_c^{S=1/2} = \frac{2J}{\log(1+\sqrt{2})} \approx 2.269$ and $T_c^{S=1} \approx 1.695$ [17,18].

3 Geometrical Properties of spin configurations

In this section we examine the geometrical properties featured by the magnetic pattern developing on the Ising lattice. In particular, we want to achieve evidence that, as noticed in [1], the distribution of up, down (and possibly zero) spins on the lattice is affected by the thermal dynamics applied to the system (Fig. 1).

Therefore, in our analysis we ought to consider not a particular, singular cluster, but rather the whole lattice. In this context, we distinguish the *positive cluster*, referred as the set of sites occupied by up spins, from *negative* and *null clusters*, analogously meant. The geometric analysis of such clusters is obtained by means of the box-counting method which, at a single blow, succeeds in taking into account the whole magnetic arrangement.

In fact, according to the box-counting technique, an r -spaced square (in general a d -dimensional box) grid is superimposed onto the object to be measured and the number of squares, $N(r)$, overlapping a portion of the object is counted. This step is repeated for different values of r . Finally, if the limit

$$d_f = \lim_{r \rightarrow 0} \frac{\log N(r)}{\log(1/r)}$$

exists, it converges to the box-counting fractal dimension d_f [19]. In other words, $N(r)$ scales as r^{-d_f} [20]. Then, once possible sources of wrong estimates removed [21], d_f

can be calculated using the linear regression technique. More precisely, d_f is assumed to be the angular coefficient of the regression line between $\log N(r)$ and $\log(1/r)$.

As remarked in [21], for an ideal fractal, such a power-law relation holds over an infinite range of scales, while, in real measures, some limits emerge. In particular, when dealing with fractal images embedded in a d -dimensional, discrete space, by taking the limit of box-size r to zero, any curve or shape on that space will have fractal dimension d . Thus, the smallest practical box-size is $r = 1$. Moreover, the range of scales can be limited by further cutoffs such as, for example, the presence of characteristic lengths and a limited volume of the object.

In the present case, clusters develop on a square lattice of side L and the spacing r is varied amongst integer submultiples of L , being 2 its minimum value (when $r = 1$ we would simply count the number of spins oriented in the same direction). Actually, there also exists a constrain from above, since (below T_c) the upper cutoff length for self-similarity is not the size of the lattice, but rather the fractal correlation length ξ . The latter is related to the characteristic cluster size so that, when $r > \xi$, each covering-box contains a portion (at least one single site) of the clusters considered. As a result, above ξ , Euclidean geometry prevails and $N(r) \sim r^d$ (where d is the lattice dimension). In other words, at scales larger ξ , the object to measure looks homogenous [22]. In the following, the fractal correlation length relevant to negative and null clusters will be referred as ξ_{-1} and ξ_0 , respectively.

In summary, our measures are carried out focusing on the proper ‘‘fractal range’’ (small scales) and, in particular, d_f is calculated with the linear regression technique over the interval $r \in [2, \xi]$.

It should as well be remarked that, when dealing with the very critical region, there exist other kinds of methods [3,4,5,6,7,8,9], specially meant, which ought to be preferred since they provide a better reliability. On the other hand, we recall that, here, our aim is not to measure the fractal dimension of the critical cluster, but rather to study the behavior of the diffusive dynamics introduced, seeking a differentiation with respect to the non-diffusive ones, in terms of geometrical properties.

The following subsection is devoted to some general observations concerning the evolution of the magnetic pattern, while a depth study of the critical range is left to the second part.

3.1 Evolution of magnetic patterns

In general, our measures refer to the magnetic configurations corresponding to the steady-states of a sample initially set ferromagnetic ($\langle m \rangle_0 = +1$) and then heated.

Figures 2 and 3 show results obtained for the spin-1/2 and spin-1 systems, respectively; because of different temperature scales, data pertaining to diffusive and non-diffusive dynamics are plotted vs the reduced temperature ($T_r = \frac{T - T_c}{T_c}$).

First of all, notice that both plots evidence a singular behavior in T_c , consistent with the phase transition oc-

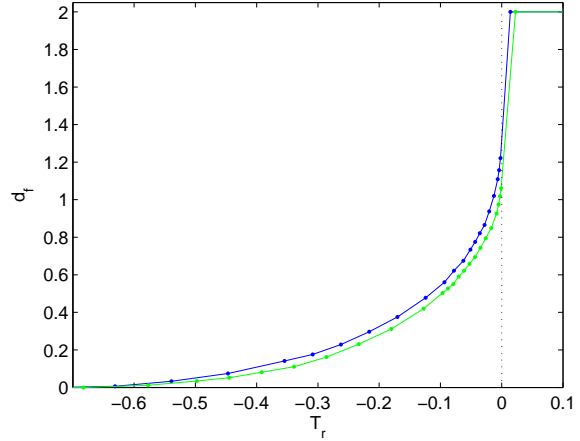


Fig. 2. Fractal dimension of negative cluster developing on an Ising lattice of linear dimension $L = 240$, made up of spin-1/2 and subject to the diffusive (dark line) and non-diffusive dynamics (clear line).

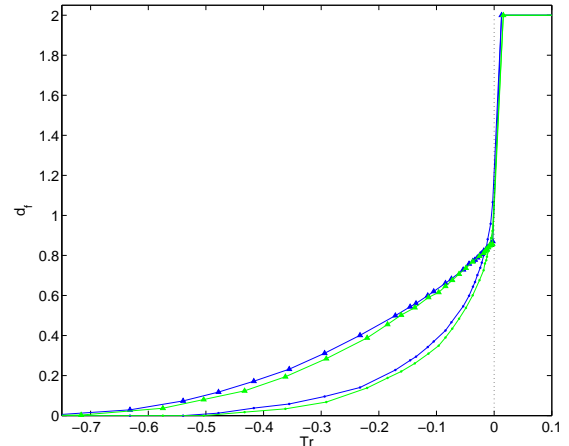


Fig. 3. Fractal dimension of magnetic clusters developing on an Ising lattice of linear dimension $L = 240$, made up of spin-1 and subject to the diffusive diffusive (dark line) and non-diffusive dynamics (clear line) Both negative (\bullet) and null (Δ) clusters are depicted.

curing on the lattice. Hence, criticality also emerges from the geometry of the spin-configuration, though observed on small scales (i.e. the fractal range).

Also notice that, for any cluster considered, for example the one labelled as ν , we can introduce the temperature τ_ν such that, if $T \leq \tau_\nu$ then $d_f(\nu) = 0$. In other words, for sufficiently low temperatures, negative and null spins are still so sparse that their fractal dimension is zero.

The consistency with the magnetic evolution of the sample is not limited to the critical point and to very low temperatures. For example, let us consider the spin-1 system of Figure 3 (an analogous description also holds when $S = 1/2$, Fig. 2). As long as $\tau_{-1(0)} < T < T_c$, the fractal dimension of negative (null) clusters increases con-

tinuously with the temperature and, finally, for $T > T_c$, d_f reaches the Euclidean dimension of the lattice. Therefore, when the paramagnetic phase is achieved, all three kinds of clusters share the same dimension. However, although the curves depicted in figure both exhibit a discontinuity at T_c , they are quite dissimilar. In particular, as will be discussed later, they display a different functional dependence on T . Besides, $\tau_{-1} > \tau_0$, due to the fact that null spins can appear on the ferromagnetic lattice at lower temperatures, because of a minor energy cost. For the same reason, at low temperatures, such spins act as catalysts for the phase transition: flips in favor of negative spins are less expensive if they engage sites adjacent to, or occupied by null spins.

As far the non diffusive dynamics (explicitly, a Glauber dynamics with type-writer updating), qualitatively similar plots have been obtained. In particular, a consistent singularity is still recorded at T_c and all fractal dimensions still converge when the reduced temperature gets positive, but, we recall, this happens at different values of T (Eq. 4 and 5).

There are other qualitative analogies between diffusive and non-diffusive dynamics, which concern the fractal correlation length. Firstly, for both dynamics, ξ grows slowly with the lattice size, especially at temperatures approaching the critical one. Consequently, in order to extend the range over which the box-counting is applied (which means more accuracy), the size L of the lattice has to be significantly enlarged. Secondly, the self-similarity range of null clusters is very small. More precisely, when $L = 240$, ξ_{-1} is about $3 \cdot 10^{-2}$ times the lattice size, while ξ_0 is about $\frac{\xi_{-1}}{2}$. In fact, because of their negligible energy contribution, null spins are not expected to form wide clusters but they are arranged throughout the whole sample, amongst positive as well as negative clusters, due to the symmetry of the system. Therefore, while heating the sample, their density increases and they form clusters whose typical size is so small, that the distribution of null spins appears to be homogenous at relatively small scales. In other words, they are more and more likely to be found in any covering box of relatively small size.

Hitherto, we have just reported the qualitatively analogies between the two dynamics taken into account. However, in the next subsection, a deeper insight will highlight some interesting differences. For the present, notice that, once the reduced temperature fixed, the diffusive dynamics introduced generates spin distributions which, compared with their non-diffusive counterparts, display a greater fractal dimension (Figs. 2 and 3). Such a difference is related to the way each thermal dynamics deals with fluctuations at small scales.

At very low temperatures, the magnetic patterns generated by the two dynamics taken into account (at the same T_r) are indistinguishable: perturbations away from the ordered background are very small (mostly made up of single sites) and they are so sparse that $d_f = 0$. By rising the temperature, their number, as well the correlation length, also increases and differences emerge.

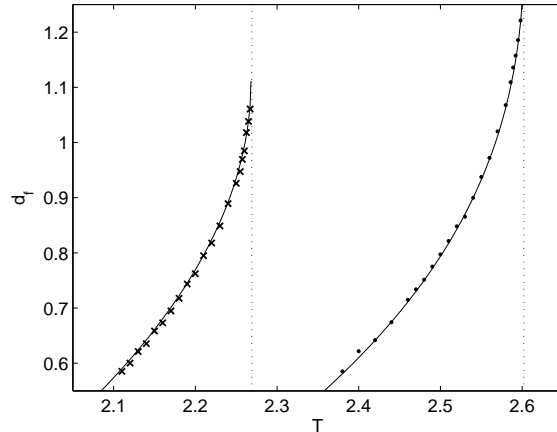


Fig. 4. Box-counting fractal dimension for the negative cluster relevant to the spin-1/2 Ising system on a squared lattice. Both kind of dynamics are depicted: non-diffusive (\times) and diffusive (\bullet). The line fitting the data is the power law of Eq. 6. The vertical, dashed lines indicate the value of the pertaining critical temperatures.

In fact, due to the bias it is endowed with, the random walker performing the diffusive dynamics is especially concerned with high energy sites. In particular, it spends most of its time on border between the largest correlated regions, while fluctuations at small scales survive quite numerous, though small-sized. On the other hand, when a non-diffusive dynamics is applied, each site is equivalently often considered for the updating so that perturbations are more likely either to grow or to be destroyed. Therefore, at small scales, correlated regions away from the ordered background are larger and sparser (Fig. 1).

As a result, when covering-boxes are counted, while reducing their size, the rate of growth of the number of boxes overlapping a negative spin is larger in the diffusive case.

3.2 Critical behavior

Now, let us focus the attention on the critical region which, in this context, is meant as the range of temperatures approaching (from below) T_c . Interestingly, for the spin-1/2 and spin-1 Ising systems taken into account (Figs. 2 and 3), d_f displays a functional dependence on T which is affected by the kind of cluster, but by neither the dynamics nor the spin magnitude. Specifically, the negative cluster is described by a power law such as:

$$d_f = d^- + A^- \left(\frac{T_c - T}{T_c} \right)^\kappa, \quad (6)$$

while the null cluster by a linear law:

$$d_f = d^0 + A^0 T, \quad (7)$$

Due to the aforesaid range of reliability of the box-counting technique, both Eq. 6 and 7 hold when $T < T_c$.

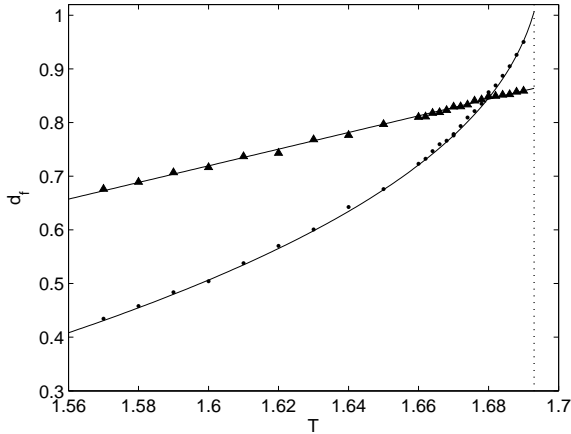


Fig. 5. Spin-1 Ising system subject to a non-diffusive dynamics. The box-counting dimension for the negative (\bullet) and null (Δ) clusters developing on the square lattice are shown. Notice the difference in their behavior with respect the temperature: they agree with the power and linear laws of Eq. 6, 7, respectively. The estimated critical temperature for this kind of system is suggested by the dashed line.

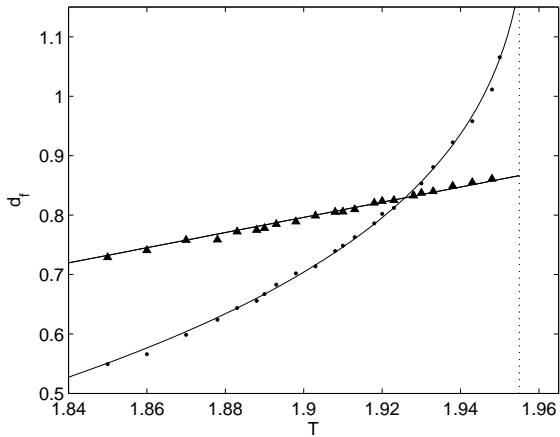


Fig. 6. Box-counting fractal dimension for the negative (\bullet) and null (Δ) clusters relevant to the spin-1 Ising system on a squared lattice; the dynamics adopted is diffusive. The lines fitting the data are a power (Eq. 6) and a linear (Eq. 7) law, respectively. The vertical, dashed line indicates the estimated value of the critical temperature.

The value of the parameters, appearing in the previous equations, have been obtained by fitting data plotted in Figures 4–6 and are resumed in Tab. 1. Notice that T_c has been regarded as a free parameter, too. Therefore, we are also able to provide a “geometrical estimate” for the critical temperature. Actually, such estimate well agrees, within the error, with its exact or measured counterpart [1]. Furthermore, it should be underlined that T_c is the most accurate among all the fitting parameters.

As far the other parameters, while d^- provides a rough estimate for the fractal dimension of the critical negative

	NDD		DD	
	$S = 1/2$	$S = 1$	$S = 1/2$	$S = 1$
d^-	1.11(7)	1.29(18)	1.41(17)	1.65(24)
A^-	-1.98(5)	-2.08(9)	-2.13(8)	-2.21(10)
κ	0.50(7)	0.34(6)	0.38(4)	0.24(4)
T_c	2.268(4)	1.698(8)	2.603(6)	1.958(1)
d^0	-1.76(3)		-1.95(3)	
A^0	1.55(2)		1.33(2)	

Table 1. Fit coefficients referring to Eq. 6 and 7, pertaining to the non-diffusive dynamics (NDD) and the diffusive dynamics introduced (DD).

cluster, we are especially interested in κ and A^0 , since they do characterize the evolution of spin arrangements. Indeed, as shown by Tab. 1, κ and A^0 depends on both the dynamics adopted and the spin magnitude S . This means that, once the dynamics (diffusive or non-diffusive) selected, the negative clusters pertaining to spin-1/2 and spin-1 systems, respectively, show a different geometric evolution. Not only, the geometric evolution of a particular cluster is also dynamic-sensitive.

This is really a non-trivial result since, from a thermodynamic point of view, the dynamics introduced actually recovers the canonical critical behavior. More precisely, the critical exponent α , β , γ have revealed to be the same, in the spin-1/2, as well as in the spin-1, 2-dimensional systems [1]. Therefore, as far the critical behavior is concerned, the very effects of our dynamics have to be tracked down in the geometry of magnetic patterns, rather than in the thermodynamic quantities.

In particular, the exponent κ pertinent to the diffusive dynamics is smaller, which means that, as $T_r \rightarrow 0^-$, the rate of growth of the fractal dimension of the related negative cluster is larger. Such phenomena are consistent with the above described effects of the diffusive, biased character of the dynamics introduced. Moreover, as you can see from Tab. 1, the same holds not only when $S = 1/2$, but also when $S = 1$. In fact, the fitting parameters of Eq. 6 display the same inequalities when diffusive and non-diffusive dynamics are compared.

On the other hand, once the thermal dynamics selected, the spin-1 system shows, with respect the $S = 1/2$ case, smaller exponents κ and larger parameters d^- . The reason is that, as previously underlined, when $T < T_c$, the presence of null spins makes the negative ones more likely to occur. In fact, due to their energetic neutrality, null spins can be spread throughout the whole lattice, at a relatively small energy cost. Now, if $\sigma_i = 0$, transitions towards $\sigma_i = -1$ or $\sigma_j = -1$ (where $i \sim j$) show significantly reduced energy costs and are therefore more likely to happen. As a result, not only negative spins are more uniformly distributed, but their number rapidly increases as $T \rightarrow T_c$.

As far the null cluster, the linear law evinced reveals that, interestingly, its evolution is indeed qualitatively different with respect the negative cluster. More precisely, its growing dynamics is slower (especially when the diffusive dynamics is applied). However, comparisons in this sense

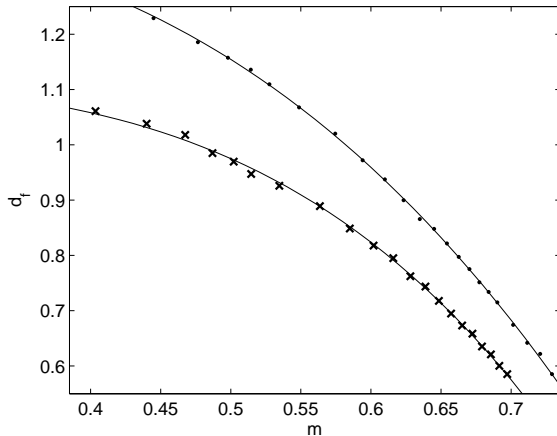


Fig. 7. Box-counting fractal dimension for the negative cluster obtained with a diffusive (\bullet) and non-diffusive (\times) dynamics applied to the spin-1/2 Ising system. The box-counting dimension is depicted as a function of the total magnetization m and the lines fitting the data can be derived from (Eq. 6). In particular, d_f scales as $m^{\frac{\kappa}{\beta}}$.

should be quite careful since, we recall, the related fractal lengths are not the same.

Some remarks are in order now. The values of the fitting parameters, especially the exponent κ , are quite sensitive to the measures of the fractal dimension d_f , just nearby the critical point. This explains the quite large errors affecting the exponents κ , which may also not forbid their overlapping. On the other hand, the power and linear laws evinced, as well as the differences displayed by the diffusive dynamics, still hold within the error.

Finally, notice that, in the analysis carried on, we could have considered d_f as a function of the total magnetization m rather than as a function of the reduced temperature T_r . However, this change would not lead to any significant differences. In fact, the power and linear laws of Eq. 6 and 7 would still hold, though their coefficients would be properly modified. This is a consequence of the aforesaid analogy between the thermodynamic critical behavior displayed by diffusive and non-diffusive dynamics. In particular, the two different dynamics would still provide different exponents κ , though rescaled by a factor β with respect to the original ones (Fig. 7).

4 Conclusions

The thermal diffusive dynamics introduced and analyzed in [1] has been further inspected, focusing the attention on the geometrical properties featured by clusters developing on the magnetic lattice. In particular, by means of the box-counting method, we measured and compared the fractal dimension of magnetic patterns generated by our diffusive dynamics and by a non-diffusive one. We have also taken into account either spin-1/2 and spin-1 systems.

As expected, in any case, when $T > T_c$ each cluster (positive, negative and, possibly, null) shows the dimen-

sion of the lattice itself. In fact, when the paramagnetic phase is reached, each kind of cluster is likely to overlap any covering-box, due to the discreteness of the lattice and to a limited number of possible spin-states. On the other hand, when $T \leq T_c$ a much more interesting scenario appears.

In general, the fractal dimension d_f of clusters displays a dependence on T consistent with the thermodynamic evolution of the magnetic lattice. In particular, in T_c , a singularity evidences the occurrence of the phase transition. Hence, criticality also emerges from the small-scales fractal geometry of magnetic patterns. Besides, as $T_r \rightarrow 0^-$, the fractal dimension of the negative cluster depends on T_r through a power law. The related fitting coefficients provide not only good estimates of the critical temperature, but they also highlight some interesting differences between the diffusive and non-diffusive dynamics. In particular, the former, as a consequence of its diffusive, biased character, generates a less sparse distribution of negative spins and then, the related fractal dimension is larger. Our data also suggest the exponent characterizing the diffusive dynamics to be smaller, which means a larger rate of growth for d_f , as approaching T_c .

Therefore, the very effects of the diffusive dynamics introduced lie in the geometrical, rather than thermodynamic [1], critical behavior of the system.

Such effects occur for both the spin-1/2 and spin-1 systems considered. Interestingly, in the latter case, negative clusters display even smaller exponents, while null clusters show a distinct behavior. In particular, their fractal dimension depends linearly on T . However, it should be underlined that the fractal range pertinent to negative and null clusters is different, being smaller for the latter. Such differences has to be attributed to the special role played by the state $\sigma = 0$. In fact, as energetically neutral, it is prevented by forming wide domains, while, at sufficiently large temperatures, it is likely to be found throughout the whole lattice. We argue that it would be worth studying to what extent such a gap among spin states affects the BRW behavior as well as the shape of clusters. For example, one could take into account systems like the q -state Potts model or the spin- S ($S > 1$) Ising model, where a different symmetry among spin-states is present.

References

1. E. Agliari, R. Burioni, D. Cassi and A. Vezzani, Eur. Phys. J. B, **46**, 109 (2005).
2. P. Buonsante, R. Burioni, D. Cassi and A. Vezzani, Phys. Rev. E, **66**, 36121 (2002), and references therein.
3. W. Janke and A.M.J. Schakel, Phys. Rev. E **71**, 36703 (2005).
4. A. Coniglio, Phys. Rev. Lett. **62**, 3054 (1989).
5. N. G. Antoniou, Y. F. Contoyiannis, and F. K. Diakonou, Phys. Rev. E **62**, 3125 (2000).
6. C. Vanderzande and A. Stella, J. Phys. A **22**, L445 (1989).
7. C. Vanderzande, J. Phys. A **25**, L75 (1992).
8. Y. Deng, H.W.J. Blöte and B. Nienhuis, Phys. Rev. E **69**, 26123 (2004).

9. B. Duplantier, Phys. Rev. Lett. **84**, 1363 (1999).
10. P. Guenoun, F. Perrot, and D. Beysens, Phys. Rev. Lett. **63**, 1152 (1989).
11. B. Han, D. Li, D. Zheng and Y. Zhou, Phys. Rev. B **66**, 14433 (2002).
12. P. Monceau and M. Perreau, Phys. Rev. B **63**, 184420 (2001).
13. J. Asikainen, A. Aharony, B.B. Mandelbrot, E. Rauch and J.-P. Hovi, Eur. Phys. J. B, **34**, 479 (2003).
14. A. Block, W. von Bloh, and H. J. Schellnhuber, Phys. Rev. A **42**, 1869 (1990).
15. B. Dubuc, J.F. Quiniou, C. Roques-Carmes, C. Tricot and S.W. Zucker, Phys. Rev. A, **39**, 1500 (1989).
16. T.C. Halsey, P. Meakin and I. Procaccia, Phys. Rev. Lett. **56**, 854 (1985).
17. W. Hoston and A.N. Berker, Rev. Lett **67**, (1991) 1027.
18. R. da Silva, N.A. Alves and J.R. Drugowich de Felício, Phys. Rev. E **66**, (2002) 26130.
19. M. Schroeder, *Fractals, Chaos, Power Laws* (W.H. Freeman and Company, New York 1991).
20. B. B. Mandelbrot, *The Fractal Geometry of Nature* (W.H. Freeman and Company, New York 1982).
21. M. Ciccotti and F. Mulargia, Phys. Rev. E **65**, 37201 (2002).
22. A. Hasmy, M. Foret, J. Pelous and R. Jullien, Phys. Rev. B **48**, 9345 (1993).

